

Hydrothermal Coating of Hydroxyapatite on ZrO₂ Ceramics

Jung-Soo Ha[†]

School of Advanced Materials Engineering, Andong National University, Kyungbuk 760-749, Korea

(Received May 31, 2006; Accepted July 30, 2006)

ABSTRACT

Hydrothermal deposition of hydroxyapatite coatings on two types of ZrO₂ substrates (3 mol% Y₂O₃-doped and 13 mol% CeO₂-doped tetragonal ZrO₂s) was studied using aqueous solutions of Ca(NO₃)₂·4H₂O and (NH₄)₂HPO₄ containing EDTA (ethylene diamine tetra acetic acid) disodium salt as a chelating agent for Ca²⁺ ions. For the precipitation of the coatings, the EDTA-Ca²⁺ chelates were decomposed by oxidation with H₂O₂ at 90°C. The deposition behavior, morphology, and orientation of the coatings were investigated while varying the solution pH using scanning electron microscopy and X-ray diffractometry. For the two substrates, sparse deposition of the coating was obtained at pH 5.5, whereas a uniform deposition was obtained at pH 7.1, 9.8, and 11.4 with a denser microstructure for the higher pH. The coating consisted of thin needle-like or plate-like crystals (1-2 μm length or diameter) at pH 7.1, but fine rod-like crystals (1-2 μm length, 0.1 μm diameter) at pH 9.8 and 11.4. The coatings were 1-3 μm thick and showed a preferred orientation of the hydroxyapatite crystals with their c axis (i.e., the elongated direction) perpendicular to the substrate surface especially for pH 9.8 and 11.4.

Key words: Hydrothermal deposition, Hydroxyapatite coatings, ZrO₂ substrates, Oxidative decomposition, Preferred orientation

1. Introduction

Hydroxyapatite, Ca₁₀(PO₄)₆(OH)₂, has attracted great concern as a biomaterial because it is very similar to the inorganic constituent of bone and teeth in composition and thus can directly bond to living tissue by a biological reaction. Due to the low strength of sintered bodies, however, it has a limitation in applications such as artificial joints and bones bearing a high load, but has wide applications in the dental field.¹⁾ Materials with a high strength and chemical stability such as Ti alloy, Al₂O₃, and ZrO₂ are biocompatible and are used in orthopedic implants, but their bioinert nature causes them to become encapsulated by a dense fibrous tissue that prevents direct bonding to soft and hard tissues in the body, leading to a loosening of the implants. Therefore it has been a big concern to overcome such a problem by the employment of bioactive hydroxyapatite coating.

Plasma spraying is the most common method for hydroxyapatite coating. Other methods such as sputtering, flame spraying, electrochemical deposition, CVD, sol-gel, pulsed laser deposition, and electrophoresis have also been used for hydroxyapatite coating. The main issues surrounding these methods are related to the decomposition of hydroxyapatite, the appearance of unidentified crystalline or amorphous phases, and the off-stoichiometry of

hydroxyapatite, all of which can be attributed to their high processing temperatures.^{1,2)} A biomimetic process using the simulated body fluid has also been attempted to produce hydroxyapatite coating at the physiological temperature (37°C).^{3,6)} A hydrothermal process can produce crystalline, compositionally homogeneous hydroxyapatite coatings without the need for high temperature calcinations.²⁾

The hydrothermal processes for hydroxyapatite coatings involve heat treatments of substrates in an aqueous solution containing Ca²⁺ and PO₄³⁻ ions in an autoclave normally above 100°C. Although there are various sources of Ca²⁺ and PO₄³⁻ to make the solution, Ca(NO₃)₂·4H₂O or CaCl₂ and (NH₄)₂HPO₄, NaH₂PO₄ or Na₂HPO₄ are commonly used to form hydroxyapatite coatings on various substrates of Ti, Ti alloy, ZrO₂, and Al₂O₃.^{3,7-10)} In this case, Ca²⁺ ions are chelated with EDTA (ethylene diamine tetra acetic acid) in order to prevent an immediate reaction with PO₄³⁻, which will precipitate hydroxyapatite powders rather than coatings before reaching the desired hydrothermal conditions during the process. For the precipitation of hydroxyapatite coatings, the EDTA-Ca²⁺ chelates are dissociated thermally^{3,7-9)} or decomposed by oxidation with H₂O₂.^{10,11)} Compared with Ti, few studies have been carried out regarding Al₂O₃.^{3,10,12,13)} and ZrO₂.³⁾ In the case of ZrO₂, a previous work³⁾ used the thermal dissociation method and observed contrary deposition behavior of hydroxyapatite coating with the substrate material type. Specifically, a uniform deposition of hydroxyapatite was obtained with a 12Ce-TZP (12 mol% CeO₂-doped tetragonal zirconia) substrate, whereas a sparse deposition with a 3Y-TZP (3 mol%

[†]Corresponding author: Jung-Soo Ha

E-mail : jsha@andong.ac.kr

Tel : +82-54-820-5637 Fax : +82-54-820-6211

Y₂O₃-doped tetragonal zirconia) substrate. Such a difference was attributed to the difference in the surface roughness of the substrates. However, this explanation seems to be unreasonable because the deposition of hydroxyapatite was done equally on as-sintered surfaces for the two substrates so that the surface roughness in both cases presumably did not differ significantly.

In the present work, the oxidative decomposition method was used to deposit hydroxyapatite coatings on two types of ZrO₂ substrates, 3Y-TZP and 13Ce-TZP (13 mol% CeO₂-doped tetragonal zirconia), under hydrothermal conditions with the solutions prepared using Ca(NO₃)₂·4H₂O and (NH₄)₂HPO₄. The deposition behavior, morphology, and orientation of the coatings were investigated with varying the solution pH using scanning electron microscopy and X-ray diffractometry.

2. Experimental Procedure

Solutions for the hydrothermal reaction were prepared using reagent-grade chemicals (Aldrich, Milwaukee, USA). Calcium nitrate (0.01 mol) was dissolved in deionized water and then EDTA disodium salt dihydrate (0.012 mol) was added to chelate the Ca²⁺ ions. After stirring the solution for 10 min, ammonium hydrogen phosphate (0.006 mol) was added to make a stock solution of 140 ml with a Ca/P atomic ratio of 1.67, which is the value for stoichiometric hydroxyapatite. The pH value of the solution was adjusted to 5.5, 7.1, 9.8, and 11.4 with NH₄OH and NaOH.

The 3Y-TZP and 13Ce-TZP substrates were prepared using two commercial ZrO₂ powders, TZ-3Y (mean particle size 0.3 μm; Tosoh Corp., Japan) and CEZ-13 (mean particle size 0.34 μm; Daiichi Kigenso Kagaku Kogyo Co., Japan), respectively, by sintering for 2 h at 1450°C to give disc-shaped substrates (10 mm in diameter by 3 mm) with a relative density of 98%. The substrate surfaces were ground with diamond plate down to 800 grit.

The hydrothermal treatments were performed in a Teflon-lined autoclave (45 ml; Parr Instrument Co., USA). In the experiments, 23 ml of the stock solution was loaded into the reaction vessel after which 3 wt% H₂O₂ was added. The substrates were suspended in the solution and the vessel was heated at 2°C/min to 90°C and held for 4 h. After the hydrothermal treatment, the substrates were washed with deionized water for 2 min in an ultrasonic bath and dried at room temperature.

The microstructures of the top surfaces and fracture surfaces of the treated substrates were observed by Scanning Electron Microscopy (SEM; JSM 6300, JEOL, Japan). The crystalline phases of the substrates and the coatings deposited were identified by X-Ray Diffraction (XRD; D/MAX-2000, Rigaku, Japan). Especially for the analysis of the coatings, a thin film mode was used with a grazing incidence angle of 1°.

3. Results and Discussion

Figs. 1 and 2 show the scanning electron micrographs of

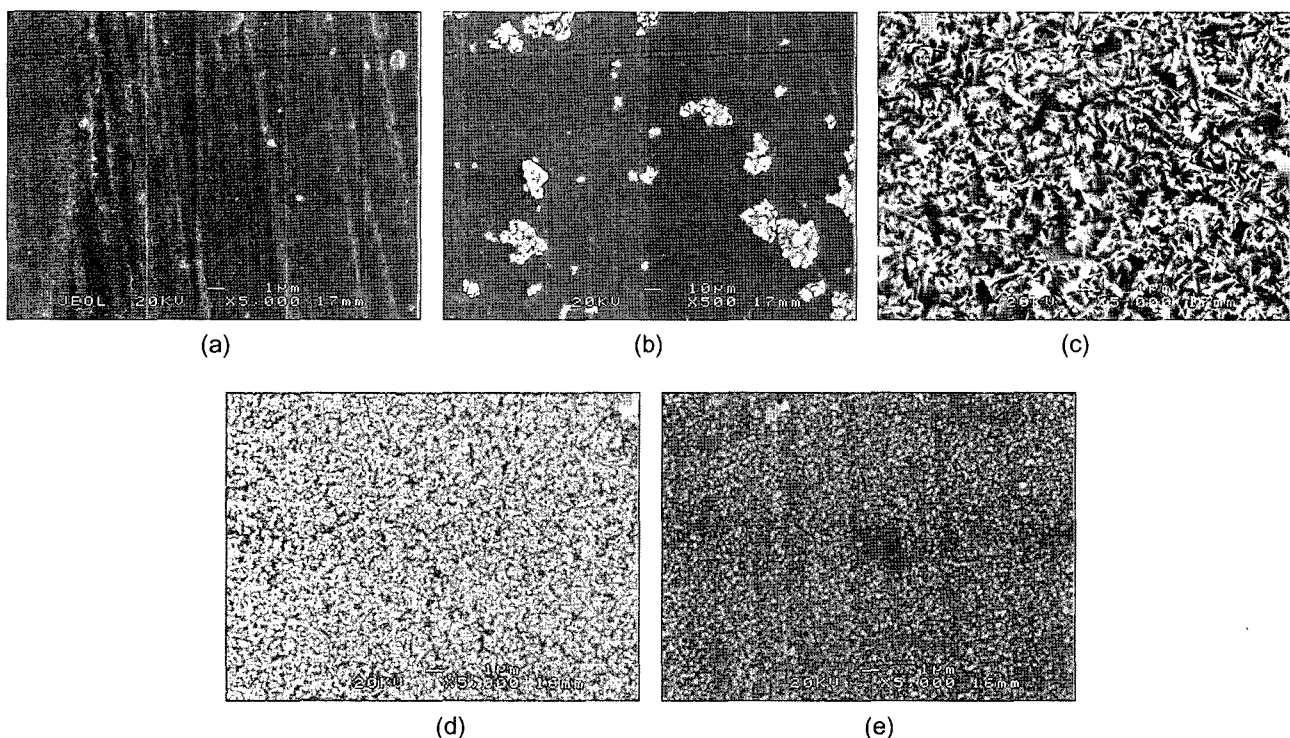


Fig. 1. Surface morphology of the 3Y-TZP substrates before and after hydrothermal treatments with varying pH condition: (a) untreated, (b) pH 5.5, (c) pH 7.1, (d) pH 9.8, and (e) pH 11.4.

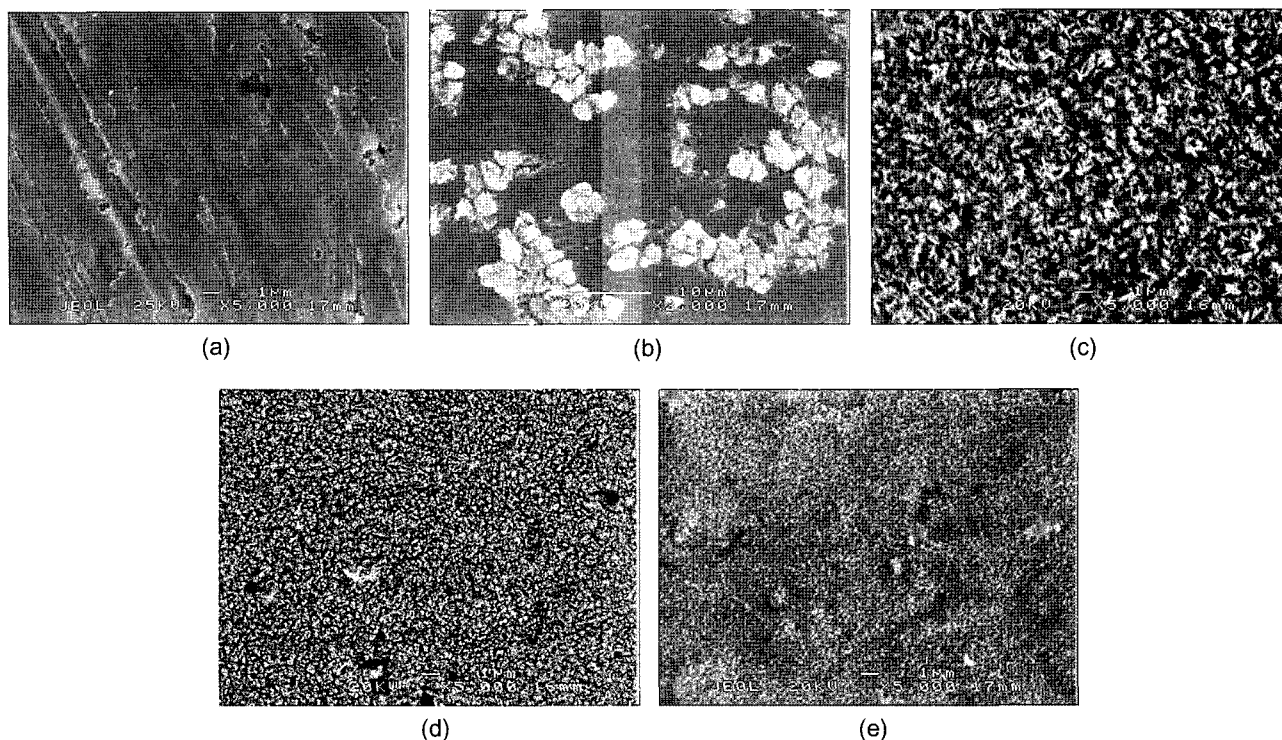


Fig. 2. Surface morphology of the ¹³Ce-TZP substrates before and after hydrothermal treatments with varying pH condition: (a) untreated, (b) pH 5.5, (c) pH 7.1, (d) pH 9.8, and (e) pH 11.4.

the surfaces of the 3Y-TZP and ¹³Ce-TZP substrates, respectively, before and after the hydrothermal treatments. The two substrates exhibited similar coating deposition behavior with the variation of the pH of the hydrothermal solution. That is, sparse deposition of the coating was obtained at pH 5.5, whereas a uniform deposition at pH 7.1, 9.8, and 11.4. Particularly when the pH was 9.8 and 11.4, the coating crystals were so fine that their size and shape could not be identified at the magnification used.

In order to find the size and shape of the coating crystals, an SEM observation at a higher magnification was performed and the results are shown in Figs. 3 and 4. In the case of the 3Y-TZP substrate (Fig. 3), it is clear that the coating consisted of thin needle-like crystals (1-2 μm length)

at pH 7.1, while it consisted of particle-like crystals (0.1-0.2 μm diameter) at pH 9.8 and 11.4. In the case of the ¹³Ce-TZP substrate (Fig. 4), the coating consisted of thin needle or plate-like crystals (1-2 μm length or diameter) at pH 7.1, while it consisted of fine rod (1-2 μm length, 0.1 μm diameter) and particle (about 0.1 μm diameter)-like crystals at pH 9.8 and 11.4, respectively.

Hydroxyapatite has a hexagonal crystal structure, and the crystals form in a fine rod shape with the longitudinal direction parallel to the *c* axis when produced hydrothermally at an alkaline pH.^{2,10} When deposited on an alumina substrate hydrothermally at pH 9.8, hydroxyapatite crystals grow into hexagonal rods with the elongated direction oriented vertically to the substrate.^{12,13} Hence, it was specu-

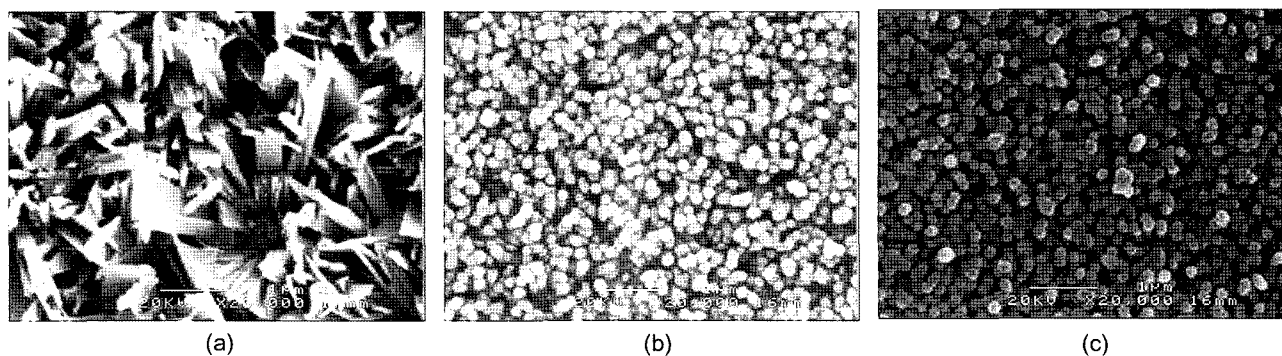


Fig. 3. Surface morphology of the coatings at a higher magnification, formed on 3Y-TZP substrates with varying pH condition: (a) pH 7.1, (b) pH 9.8, and (c) pH 11.4.

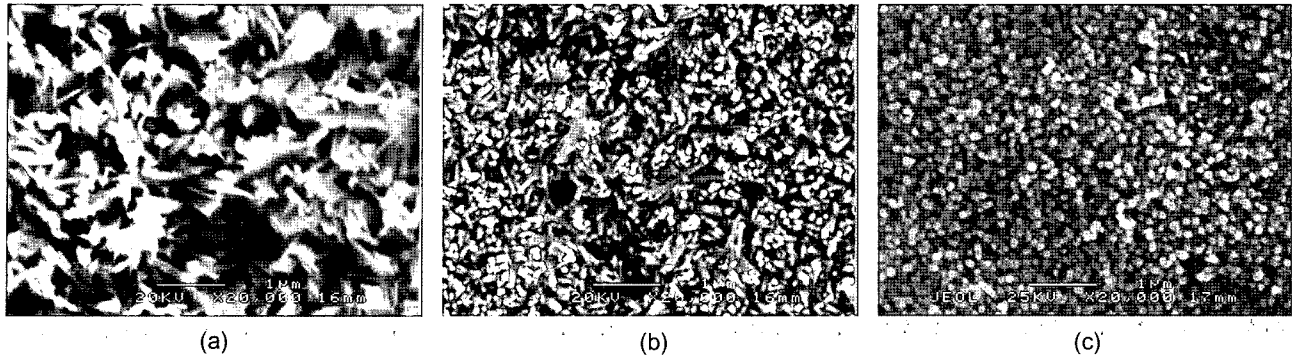


Fig. 4. Surface morphology of the coatings at a higher magnification, formed on 3Y-TZP substrates with varying pH condition: (a) pH 7.1, (b) pH 9.8, and (c) pH 11.4.

lated that the images of the particle-like crystals observed for the 3Y-TZP (pH 9.8 and 11.4; Fig. 3) and 13Ce-TZP (pH 11.4; Fig. 4) substrates resulted from the vertical alignment of rod-like crystals of the coatings. This speculation is supported by the fact that the rod shape of the coating crystals could be observed due to some deviation from the vertical alignment particularly with pH 9.8 for the 13Ce-TZP substrate (Fig. 4).

The dissimilar deposition behaviors of the coatings with different pH values discussed above may be explained in terms of the Isoelectric Point (IEP) of the substrate and the number of nucleation sites for the coating. According to a previous work,¹⁴ the nucleation of hydroxyapatite starts with the adhesion of Ca^{2+} ions onto the negatively-charged surfaces of the substrate. The IEP of ZrO_2 occurs at pH 4-5,¹⁵ hence the surface charges of the substrates for the pH values under investigation here are negative, and the number of the negatively-charged sites will increase as the pH varies from 5.5 to 11.4. Especially for pH 5.5, the number of the sites is very few due to the pH close to the IEP. As the negative surface sites correspond to the nucleation sites of the coating, it is natural that a sparse deposition of the coating was obtained at pH 5.5, while a more uniform and denser deposition of the coating was obtained by increasing the pH from 7.1 to 11.4.

Fig. 5 shows the results of SEM observation of coating lay-

ers deposited on the 3Y-TZP substrate, taken using fracture surfaces of the samples. For pH 7.1, we can see that the needle-like crystals were deposited with their length upward and the coating layer was 2-3 μm thick. For pH 9.8 and 11.4, the coatings were 1-2 μm thick.

Fig. 6 shows the XRD results of the two substrates before hydrothermal treatments, confirming that they were mainly tetragonal ZrO_2 . The standard XRD pattern (JCPDS 9-432) of hydroxyapatite is also given in Fig. 6 for comparison with the XRD results of the coated samples. In order to identify the crystalline phases of the coatings obtained, thin-film XRD analyses were performed on several selected samples exhibiting uniform deposition of coatings. These were the samples prepared at pH 7.1, 9.8, and 11.4 on the 3Y-TZP substrates. The results are given in Fig. 7. Hydroxyapatite peaks were detected along with ZrO_2 peaks for all of the samples, confirming that the coatings were hydroxyapatite. It is notable that the relative intensity of hydroxyapatite peaks to the ZrO_2 peaks increased as the pH increased. This can be attributed to the denser microstructure of the hydroxyapatite coating with a higher pH, as shown in Fig. 5. Unlike the standard XRD pattern with the strongest peak intensity for (211) reflection at $2\theta = 31.8^\circ$ (Fig. 6), the coatings had the strongest peak (002) at 25.9° with a tendency that the intensity difference between this peak and the others became much

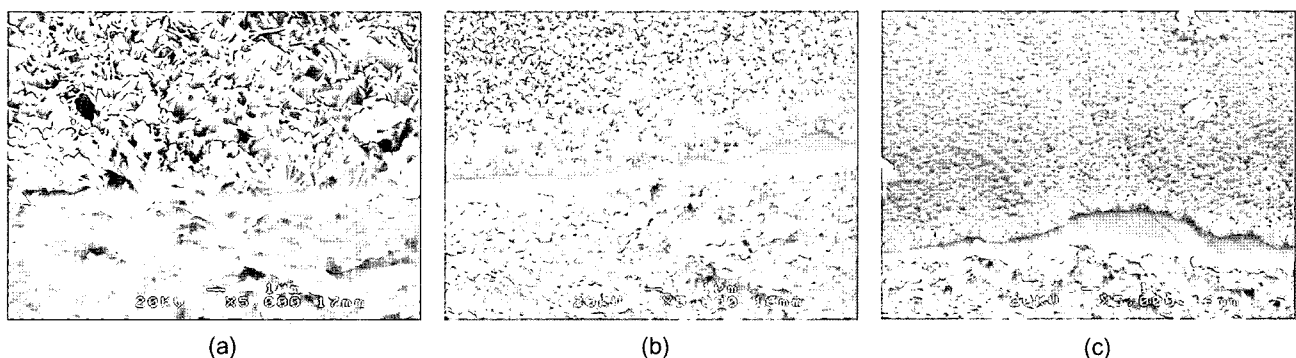


Fig. 5. Fracture surfaces of the samples of 3Y-TZP after hydrothermal treatments showing the coating layers formed on the substrates with varying pH condition: (a) pH 7.1, (b) pH 9.8, and (c) pH 11.4.

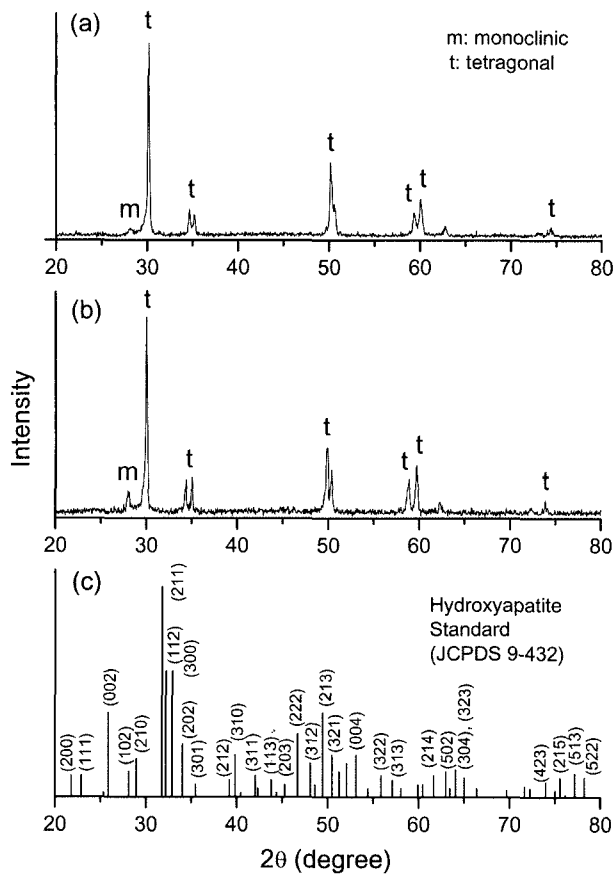


Fig. 6. XRD patterns of (a) 3Y-TZP and (b) 13Ce-TZP substrates before hydrothermal treatments along with a standard pattern of hydroxyapatite.

larger as the pH increased (Fig. 7). Such a result indicates a preferred orientation of the rod-like hydroxyapatite crystals with their *c* axis (i.e., the elongated direction) nearly perpendicular to the substrate surface especially for the high pH values of 9.8 and 11.4. This supports the earlier discussion regarding the results of SEM observations in Figs. 3 and 4. According to a previous report,¹⁶ the (*h*00) surface of hydroxyapatite mainly consists of positively charged Ca sites, whereas the (00*l*) surface consists mainly of negatively charged P sites. As mentioned earlier, the surface charge of the substrate becomes more negative as the pH increases, hence more positive Ca ions adhere to the substrate. In this situation, the (00*l*) surface with the negatively charged P sites could form readily, resulting in the preferred orientation in the [002] direction.

A preferred orientation in the [002] direction was also reported in some other works concerning hydroxyapatite coatings on metal substrates formed under hydrothermal conditions.^{17,18} This was also found in the coating on an Al₂O₃ substrate and the reaction layers of hydroxyapatite on bioglass produced using simulated body fluids,^{4,19} and in the coating on a mild steel by a thermal spraying technique.²⁰

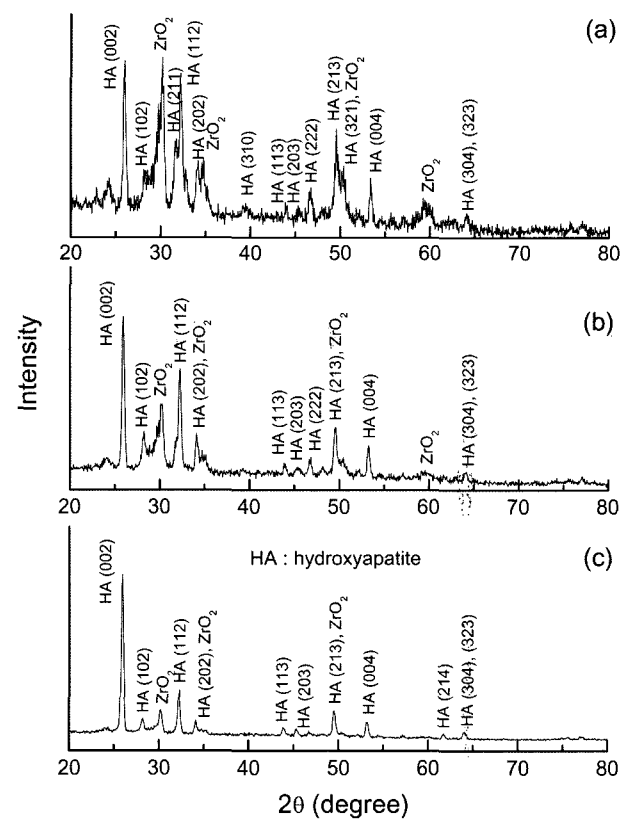


Fig. 7. XRD patterns of the samples of 3Y-TZP after hydrothermal treatments with varying pH condition: (a) pH 7.1, (b) pH 9.8, and (c) pH 11.4.

4. Conclusions

The deposition of hydroxyapatite coatings on ZrO₂ substrates was found to be dependent on the pH of the hydrothermal solution. For both the 3Y-TZP and 13Ce-TZP substrates, a sparse deposition of the coating was obtained at pH 5.5, whereas a uniform deposition was obtained at pH 7.1, 9.8, and 11.4 with a denser microstructure as the pH increased. The coating consisted of thin needle-like or plate-like crystals (1-2 μm length or diameter) at pH 7.1, while consisting of fine rod-like crystals (1-2 μm length, 0.1 μm diameter) at pH 9.8 and 11.4. The coatings were 1-3 μm thick and showed a preferred orientation of the hydroxyapatite crystals with their *c* axis (i.e., the elongated direction) perpendicular to the substrate surface especially for pH 9.8 and 11.4.

Acknowledgment

This work was supported by Andong National University through the academic research support program for 2003.

REFERENCES

1. W. Suchanek and M. Yoshimura, "Processing and Properties of Hydroxyapatite-Based Biomaterials for Use as a

- Hard Tissue Replacement Implants," *J. Mater. Res.*, **13** [1] 94-117 (1998).
2. M. Yoshimura and H. Suda, "Hydrothermal Processing of Hydroxyapatite: Past, Present, and Future," pp. 45-72 in *Hydroxyapatite and Related Materials*. Ed. by P. W. Brown and B. Constantz, CRC Press, Boca Raton, Ann Arbor, London, Tokyo, 1994.
 3. Y. Fujishiro, M. Nishino, A. Sugimori, A. Okuwaki, and T. Sato, "Coating of Hydroxyapatite on Various Substrates via Hydrothermal Reactions of $\text{Ca}(\text{edta})^{2-}$ and Phosphate," *J. Mater. Sci.: Mater. in Med.*, **12** 333-37 (2001).
 4. K. Hata, T. Kokubo, T. Nakamura, and T. Yamamura "Growth of a Bonelike Apatite Layer on a Substrate by a Biomimetic Process," *J. Am. Ceram. Soc.*, **78** [4] 1049-53 (1995).
 5. T. Kokubo, F. Miyaji, H.-M. Kim, and T. Nakamura, "Spontaneous Formation of Bonelike Apatite Layer on Chemically Treated Titanium Metals," *J. Am. Ceram. Soc.*, **79** [4] 1127-29 (1996).
 6. H.-M. Kim, H. Takadama, F. Miyaji, T. Kokubo, S. Nishiguchi, and T. Nakamura, "Mechanism of Apatite Formation on Bioactive Titanium Metal," *Kor. J. Ceram.*, **4** [4] 336-39 (1998).
 7. Y. Fujishiro, A. Fujimoto, T. Sato, and A. Okuwaki, "Coating of Hydroxyapatite on Titanium Plates Using Thermal Dissociation of Calcium-EDTA Chelate Complex in Phosphate Solutions under Hydrothermal Conditions," *J. Coll. Interface Sci.*, **173** 119-27 (1995).
 8. Y. Fujishiro, N. Sato, S. Uchida, and T. Sato, "Coating of CaTiO_3 on Titanium Substrates by Hydrothermal Reactions Using Calcium-Ethylene Diamine Tetra Acetic Acid Chelate," *J. Mater. Sci. Mater. Med.*, **9** 363-67 (1998).
 9. M. Z. Najdoski, P. Majhi, and I. S. Grozdanov, "A Simple Chemical Method for Preparation of Hydroxyapatite Coatings on $\text{Ti}_6\text{Al}_4\text{V}$ Substrate," *J. Mater. Sci. Mater. Med.*, **12** 479-83 (2001).
 10. M. Toriyama, Y. Kawamoto, T. Suzuki, Y. Yokogawa, K. Nishizawa, F. Nagata, and M. R. Mucalo, "Hydroxyapatite Coating on Alumina Ceramics by an Oxidative Decomposition Method of EDTA-Calcium Chelate," *J. Mater. Sci. Lett.*, **15** 179-81 (1996).
 11. M. Toriyama, Y. Kawamoto, T. Suzuki, Y. Yokogawa, K. Nishizawa, and H. Nagae, "Synthesis of Hydroxyapatite by an Oxidative Decomposition Method of Calcium Chelate," *J. Ceram. Soc. Jpn.*, **100** [7] 950-54 (1992).
 12. J.-S. Ha and M. N. Rahaman, "Formation of Hydroxyapatite Coatings on Alumina under Hydrothermal Conditions," *Ceram. Eng. Sci. Proc.*, **24** [3] 239-44 (2003).
 13. J.-S. Ha, "Hydroxyapatite Coating on Al_2O_3 by Hydrothermal Process," *J. Kor. Ceram. Soc.*, **40** [12] 1154-58 (2003).
 14. H. Takadama, H.-M. Kim, T. Kokubo, and T. Nakamura, "Mechanism of Biomineralization of Apatite on a Sodium Silicate Glass: TEM-EDX Study *In Vitro*," *Chem. Mater.*, **13** 1108-13 (2001).
 15. J. S. Reed, "Principles of Ceramics Processing," pp. 152, John Wiley & Sons, New York, 1995.
 16. K. Ohta, H. Monma, and S. Takahashi, "Adsorption Characteristics of Proteins on Calcium Phosphates Using Liquid Chromatography," *J. Biomed. Mater. Res.*, **55** 409-14 (2001).
 17. M. Z. Najdoski, P. Majhi, and I. S. Grozdanov, "A Simple Chemical Method for Preparation of Hydroxyapatite Coatings on $\text{Ti}_6\text{Al}_4\text{V}$ Substrate," *J. Mater. Sci. Mater. Med.*, **12** 479-83 (2001).
 18. Y. Fujishiro, T. Sato, and A. Okuwaki, "Coating of Hydroxyapatite on Metal Plates Using Thermal Dissociation of Calcium-EDTA Chelate in Phosphate Solutions under Hydrothermal Conditions," *J. Mater. Sci. Mater. Med.*, **6** 172-76 (1995).
 19. R. J. C. Knowles and W. Bonfield, "Analysis of *In Vitro* Reaction Layers Formed on Bioglass Using Thin-Film X-Ray Diffraction and ATR-FTIR Microspectroscopy," *J. Biomed. Mater. Res.*, **41** 162-66 (1998).
 20. C. M. Roome and C. D. Adam, "Crystallite Orientation and Anisotropic Strains in Thermally Sprayed Hydroxyapatite Coatings," *Biomaterials*, **16** 691-96 (1995).